Interaction between Aβ(1−42) and Aβ(1−40) in Alzheimer's β-Amyloid Fibril Formation in Vitro†

Kazuhiro Hasegawa,‡,§ Itaru Yamaguchi,‡ Saburou Omata,§ Fumitake Gejyo,|| and Hironobu Naiki*,‡

Department of Pathology, Fukui Medical University, Fukui 910-1193, Japan, Department of Biosystem Science, Graduate School of Science and Technology, Niigata University, Niigata 950-2181, Japan, and Department of Medicine (II), Niigata University School of Medicine, Niigata 951-8510, Japan

Received May 20, 1999; Revised Manuscript Received August 17, 1999

ABSTRACT: We analyzed the interaction of two kinds of amyloid β-peptides (Aβ), i.e., Aβ(1−42) and Aβ(1−40), in the kinetics of β-amyloid fibril (fAβ) formation in vitro, based on a nucleation-dependent polymerization model using fluorescence spectroscopy with thioflavin T. When 25 μM Aβ(1−42) was incubated with increasing concentrations of amyloidogenic Aβ(1−40), the time to proceed to equilibrium was extended dose-dependently. A similar inhibitory effect was observed when 45 μM Aβ(1−40) was incubated with increasing concentrations of Aβ(1−42). On the other hand, when 50 μM of non-amyloidogenic Aβ(1−40) was incubated with Aβ(1−42) at a molar ratio of 10:1 or 5:1, Aβ(1−42) initiated fAβ formation from Aβ(1−40). The lag time of the reaction shortened in a concentration-dependent manner, with Aβ(1−42). We next examined the seeding effect of fAβ formed from Aβ(1−42) (fAβ(1−42)) on nonamyloidogenic Aβ(1−40). When 50 μM of nonamyloidogenic Aβ(1−40) was incubated with 10 or 20 μg/mL (2.2 or 4.4 μM) of fAβ(1−42), the fluorescence showed a sigmoidal increase. The lag time of the reaction was shortened by fAβ(1−42) in a concentration-dependent manner. However, the time to proceed to equilibrium was much longer than when an equal concentration of fAβ formed from Aβ(1−40) (fAβ(1−40)) was added to Aβ(1−40). The fluorescence increased hyperbolically without a lag phase when 25 μM Aβ(1−42) was incubated with 10 or 20 μg/mL (2.3 or 4.6 μM) of fAβ(1−40), and proceeded to equilibrium more rapidly than without fAβ(1−40). An electron microscopic study indicated that the morphology of fAβ formed is governed by the major component of fresh Aβ peptides in the reaction mixture, not by the morphology of preexisting fibrils. These results may indicate the central role of Aβ(1−42) for fAβ deposition in vivo, among the different coexisting Aβ species.

The intracerebral accumulation of the amyloid β-peptides (Aβ)[1] as senile plaques or vascular amyloid is one of the dominant characteristics in the pathogenesis of Alzheimer's disease (AD) (*1*). The apparent role of Aβ, especially Aβ(1−42), is now considered as a unifying pathological feature of genetically diverse forms of AD (*2*). Rumble et al. (*3*) suggested that, in patients with Down's syndrome (trisomy 21) where the gene for β-amyloid precursor protein (βAPP) is present in triplicate, overexpression of this gene may lead to increased levels of βAPP and eventually cause Aβ deposition. A mutant βAPP (Lys 670-Met 671 to Asn-Leu) has been linked to a type of autosomal-dominant familial Alzheimer's disease (FAD) and suggested to cause AD by altering its own processing such that increased amounts of Aβ peptides are released (*4, 5*). In addition, mutations that increase the Aβ(1−42) level also cause AD. Mutant βAPPs (Val717 to Ile, Phe, or Gly) are linked to certain types of autosomal-dominant FAD and have been suggested to cause AD by altering the processing of βAPP in a way to release increased amounts of Aβ(1−42) (*6*). Presenilin 1 and 2 are pathogenic genes linked to autosomal-dominant FAD pedigrees. Mutations of the presenilin genes have been reported to elevate the Aβ(1−42)/Aβ(1−40) ratio both in vitro and in vivo as well as in the plasma of affected members of presenilin-linked FAD pedigrees (*7, 8*).

Several groups proposed a nucleation-dependent polymerization model to explain the mechanisms of β-amyloid fibril (fAβ) formation in vitro (*9*−*15*). This model consists of two phases, i.e., nucleation and extension phases. Nucleus formation requires a series of association steps of monomers that are thermodynamically unfavorable, representing the rate-limiting step in amyloid fibril formation. Once the nucleus (n-mer) has been formed, further addition of monomers becomes thermodynamically favorable, resulting in a rapid extension of amyloid fibrils. We and other groups have independently developed a first-order kinetic model of fAβ extension in vitro and confirmed that the extension of fAβ proceeds via the consecutive association of Aβ onto the

† This research was supported in part by Grant-in-Aid 08670242, 10670198 for Scientific Research (C) from the Ministry of Education, Science, Sports and Culture of Japan.

* Corresponding author. Tel.: 081-776-61-8320. Fax: 081-776-61-8123. E-mail: naiki@fmsrsa.fukui-med.ac.jp.

‡ Fukui Medical University.

§ Niigata University.

|| Niigata University School of Medicine.

[1] Abbreviations: Aβ, amyloid β-peptides; AD, Alzheimer's disease; apoE, apolipoprotein E; βAPP, β-amyloid precursor protein; fAβ, β-amyloid fibrils; CD, circular dichroism; ESI, electrospray ionization; fAβ(1−40), fAβ formed from Aβ(1−40); fAβ(1−42), fAβ formed from Aβ(1−42); FAD, familial Alzheimer's disease; MS, mass spectrometry; ThT, thioflavin T.

10.1021/bi991161m CCC: $18.00
Published on Web 11/04/1999

ends of existing fibrils (*12*, *15*, *16*). A characteristic sigmoidal time-course curve of fAβ formation from Aβ at a physiological pH is widely believed to represent the essence of a nucleation-dependent polymerization model, i.e., an initial lag phase represents the thermodynamically unfavorable nucleus formation (*11*).

Jarrett et al. (*9*) performed turbidimetric studies on the kinetics of fAβ formation from Aβ using synthetic naturally occurring Aβ variants [Aβ(1−39), Aβ(1−40), and Aβ(1−42)] and four model peptides [Aβ(26−39), Aβ(26−40), Aβ(26−42), and Aβ(26−43)]. They suggested that fAβ formation is a nucleation-dependent phenomenon, i.e., Aβ(1−39) or Aβ(1−40) fibrillogenesis can be nucleated by peptides with a longer C-terminal residue, for example, Aβ(1−42). They demonstrated that preformed fAβ(1−42) can nucleate the amyloidogenesis of Aβ(1−40) (seeding effect). However, the ability of fresh Aβ with a longer C-terminal residue to initiate fAβ formation from fresh Aβ with a shorter C-terminal residue was demonstrated only with two nonnaturally occurring shorter model peptides, i.e., Aβ(26−43) and Aβ(26−40). Moreover, they did not consider the kinetic interaction of different Aβ species [e.g., Aβ(1−42) and Aβ(1−40)] in the nucleation and extension processes.

In this paper, we characterized the interaction between Aβ(1−42) and Aβ(1−40) in the kinetics of fAβ formation in vitro. Two kinetic assay systems were used, i.e., the fibril extension assay and the fibril formation assay using fresh Aβ. The former virtually represents the extension phase, while the latter represents both the nucleation and extension phases. In the fibril extension assay, we incubated fAβ formed from Aβ(1−40) [fAβ(1−40)] with Aβ(1−42) or fAβ formed from Aβ(1−42) [fAβ(1−42)] with Aβ(1−40). In the fibril formation assay, we mixed Aβ(1−42) and Aβ(1−40). We propose a model for the interaction between Aβ(1−42) and Aβ(1−40) in fAβ formation in vitro.

EXPERIMENTAL PROCEDURES

Preparation of Aβ and fAβ Solutions. Aβ(1−42) (Lot No. 511908, Bachem AG, Bubendorf, Switzerland) was dissolved by brief vortexing in ice-cold 0.02% ammonia solution at a concentration of about 250 μM (1.1 mg/mL) in a 4 °C room. Although the solution was clear, short fibrils were observed by electron microscopy (data not shown). Significant thioflavin T (ThT) fluorescence was also detected by fluorescence spectroscopy. To remove these fibrils, the solution (0.8 mL) was applied to polycarbonate tubes (size 11 × 34 mm, Code No. 343778, Beckman, Palo Alto, CA) and ultracentrifuged at 10^5 g or 2×10^5 g for 3 h at 4 °C using a Beckman Optima TLX tabletop ultracentrifuge and a Beckman TLA-120.2 fixed angle rotor. The increased ultracentrifugation force reduced the rate of fAβ(1−42) formation from fresh Aβ(1−42). However, characteristic sigmoidal time-course curves were observed in both cases (data not shown). Although no visible pellets were formed after ultracentrifugation, the ThT fluorescence was collected to the bottom quarter fraction, and no significant fluorescence was detected in the upper three-quarters fraction. By electron microscopy, no fibrillar components were observed in the upper three-quarters fraction. Therefore, the upper three-quarters fraction was collected by careful aspiration and stored at −80 °C before assaying [fresh Aβ(1−42) solution]. The protein concentration of this fraction, as measured by the method described below, was 90−93% of that of the whole solution before ultracentrifugation. Aβ(1−40) (Lot Nos. 518765 and 519599, Bachem AG, Bubendorf, Switzerland) was dissolved by brief vortexing in 0.02% ammonia solution at a concentration of about 500 μM (2.2 mg/mL) in a 4 °C room and stored at −80 °C before assaying [fresh Aβ(1−40) solution]. The solution was clear, and few fibrillar components were observed by electron microscopy (data not shown). No significant ThT fluorescence was detected by fluorescence spectroscopy. Therefore, we did not perform the ultracentrifugation of Aβ(1−40) solution. Aβ(1−40) from a different vendor (Lot No. 480511, Peptide Institute, Inc., Osaka, Japan) was also treated as described above.

fAβ(1−42) were formed from the above-described fresh Aβ(1−42) solution ultracentrifuged at 10^5 g. The reaction mixture in an Eppendorf tube was 950 μL and contained 25 μM Aβ(1−42), 50 mM phosphate buffer, pH 7.5, and 100 mM NaCl. After briefly vortexed, the mixture was incubated at 37 °C for 6 h for polymerization reactions. The reaction tubes were not agitated during the reaction. After incubation, the mixture was centrifuged at 4 °C for 3 h at 1.6×10^4 g, using a high-speed microrefrigerated centrifuge (MRX-150, Tomy, Tokyo, Japan). More than 95% of fAβ(1−42) had precipitated as measured by the fluorescence of ThT. The pellet was resuspended in 50 mM phosphate buffer, pH 7.5, 100 mM NaCl, and 0.05% NaN_3 in an Eppendorf tube; sonicated on ice with 15 intermittent pulses (pulse, 0.6 s; interval, 0.4 s; output level, 2) using an ultrasonic disruptor (UD-201, Tomy, Tokyo, Japan) equipped with a microtip (TP-030, Tomy, Tokyo, Japan); and stored at 4 °C before assaying. fAβ(1−40) were formed from the above-described fresh Aβ(1−40) solution (Lot No. 519599, Bachem AG). The reaction mixture was 600 μL and contained 50 μM Aβ(1−40), 50 mM phosphate buffer, pH 7.5, and 100 mM NaCl. After incubation at 37 °C for 24 h, the mixture was centrifuged at 4 °C for 3 h at 1.6×10^4 g. fAβ(1−40) had precipitated completely as measured by the fluorescence of ThT. The pellet was resuspended in 50 mM phosphate buffer, pH 7.5, 100 mM NaCl, and 0.05% NaN_3; sonicated as described above; and stored at 4 °C before assaying.

Fluorescence Spectroscopy. All studies were performed essentially as described elsewhere (*12*) on a Hitachi F-3010 fluorescence spectrophotometer. Optimum fluorescence measurements of fAβ were obtained at the excitation and emission wavelengths of 446 and 490 nm, respectively, with the reaction mixture containing 5 μM ThT (Wako Pure Chemical Industries, Ltd., Osaka, Japan) and 50 mM glycine−NaOH buffer, pH 8.5. Fluorescence was measured immediately after making the mixture and was averaged for the initial 5 s.

Polymerization Assay. Reaction mixtures were prepared on ice at 4 °C, with neither polymerization nor depolymerization of fAβ being observed by fluorometric analysis. Distilled water was put into a tube. Then 500 mM phosphate buffer, pH 7.5, was added to yield a final buffer concentration of 50 mM, and 5 M NaCl was added to a final concentration of 100 mM. Fresh Aβ solutions were added to yield a final Aβ concentration of 5−35 μM [Aβ(1−42)] or 5−60 μM [Aβ(1−40)]. Unless otherwise noted, Aβ(1−42) ultracentrifuged at 10^5 g was used. Finally, the fAβ solution was added to yield a final fAβ concentration of 10 or 20 μg/mL

[fAβ(1−42), equivalent to 2.2 or 4.4 μM Aβ(1−42); fAβ-(1−40), equivalent to 2.3 or 4.6 μM Aβ(1−40)]. After briefly being vortexed, 30-μL aliquots of the mixture were put into oil-free PCR tubes (size 0.5 mL, Code No. 9046, Takara Shuzo Co. Ltd., Otsu, Japan). The reaction tubes were then transferred into a DNA thermal cycler (PJ480, Perkin-Elmer Cetus, Emeryville, CA). Starting at 4 °C, the plate temperature was elevated at maximal speed to 37 °C. Incubation times ranged between 0 and 21 days (as indicated in each figure), and the reaction was stopped by placing the tubes on ice. The reaction tubes were not agitated during the reaction. Three 5-μL aliquots from each reaction tube were subjected to fluorescence spectroscopy, and the mean of each triplicate was determined.

Electron Microscopy. Reaction mixtures were spread on carbon-coated grids, negatively stained with 1% phosphotungstic acid, pH 7.0, and examined under a Hitachi H-7000 electron microscope with an acceleration voltage of 75 kV.

Mass Spectrometry. The Aβ(1−40) solution was lyophilized. The Aβ(1−42) solution was dialyzed against 0.5% acetic acid at 4 °C with Spectra/Por CE DispoDialyzer (molecular weight cutoff of 1000, Spectrum Laboratories, Inc., Laguna Hills, CA). Acetic acid and acetonitrile were then added to each Aβ preparation to obtain final concentrations of 0.5 M and 50% (v/v), respectively. Samples were analyzed by TSQ-7000 mass spectrometer (Finnigan Corporation, San Jose, CA) with electrospray ionization (ESI/MS).

Secondary Structure Analysis. Secondary structure of Aβ peptides were analyzed by circular dichroism (CD). The Aβ solutions were diluted to 25 μM with 50 mM phosphate buffer, pH 7.5. The CD spectra were recorded at 8 °C using a 1.0-mm path length cell on a Jasco 725W spectropolarimeter (Jasco Corporation, Hachioji, Japan). Five accumulative readings at 1 nm bandwidth, resolution at 0.2 nm, sensitivity at 20 mdeg, response time of 2 s, and scan speed at 50 nm/min were taken from each sample, averaged, and baseline subtracted. Results were expressed in terms of mean residue ellipticity and ranged from 240 to 190 nm. The content of secondary structure was estimated by the least-squares curve-fitting method using reference spectra by Reed and Reed (*17*).

Other Analytical Procedures. Protein concentrations of the Aβ and fAβ solutions were determined by the method of Bradford (*18*), using a protein assay kit (500-0001, Bio-Rad Laboratories, Inc., Hercules, CA). Throughout this study, the Aβ(1−40) solution quantified by amino acid analysis was used as the standard. Equal amounts of Aβ(1−42) and Aβ-(1−40) quantified by amino acid analysis gave similar absorbance.

RESULTS

Characterization of Aβ Peptides. We first characterized the molecular weight of Aβs with ESI/MS. When Aβ(1−42) ultracentrifuged at 10^5 g was analyzed, a major peak was detected at 4513 [the theoretical value of intact Aβ(1−42) was 4514.16]. When three lots of Aβ(1−40)s used in this study were analyzed, a major peak was detected at 4329 in all cases [the theoretical value of intact Aβ(1−40) was 4329.9]. The peaks corresponding to methionine oxidization and deamidation were not observed in all Aβ preparations. We then analyzed the secondary structure of Aβs by CD. The β-sheet contents of Aβ(1−42) ultracentrifuged at 10^5 and 2×10^5 g were 31.7 and 29.2%, respectively. The β-sheet contents of amyloidogenic (Lot No. 519599) and nonamyloidogenic (Lot No. 518765) Aβ(1−40) were 25.2 and 24.5%, respectively. All of these Aβs did not contain α-helix.

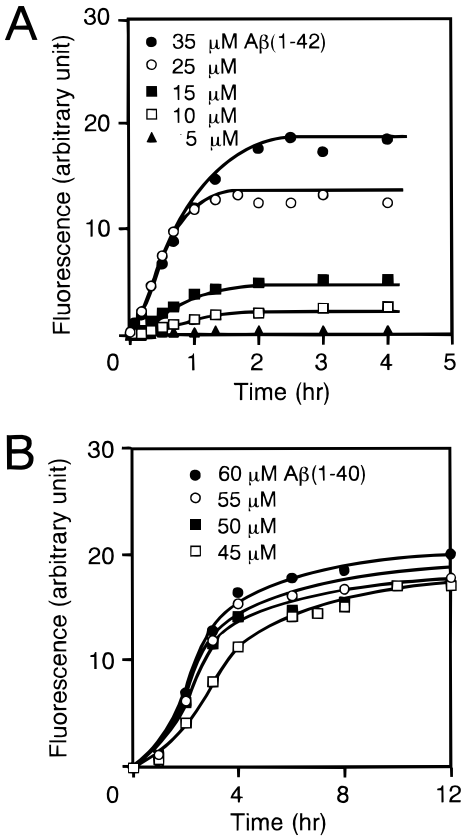

FIGURE 1: Effect of Aβ concentrations on the kinetics of fAβ formation. (A) Time course of the fluorescence after the initiation of fAβ(1−42) formation from fresh Aβ(1−42). The reaction mixture contained 50 mM phosphate buffer, pH 7.5, 100 mM NaCl, and 5 (▲), 10 (□), 15 (■), 25 (○), or 35 μM (●) Aβ(1−42). The reaction was initiated by shifting the temperature to 37 °C as described under Experimental Procedures. At each incubation time, the reaction was stopped and analyzed by fluorescence spectroscopy as described under Experimental Procedures. (B) Time course of the fluorescence after the initiation of fAβ(1−40) formation from fresh Aβ(1−40). The reaction mixture contained 50 mM phosphate buffer, pH 7.5, 100 mM NaCl, and 45 (□), 50 (■), 55 (○), or 60 μM (●) Aβ(1−40) (Lot No. 519599, Bachem AG).

Interaction between Aβ(1−42) and Aβ(1−40) in the Kinetics of fAβ Formation from Fresh Aβ. As shown in Figure 1A,B, when fresh amyloidogenic Aβ(1−42) or Aβ(1−40) (Lot No. 519599, Bachem AG) was incubated at 37 °C, the fluorescence of ThT followed a sigmoidal curve with a point of inflection. The final equilibrium level increased in a concentration-dependent manner with Aβ peptides. The time to proceed to equilibrium level of fluorescence was unchanged by the initial Aβ concentrations examined.

The interaction between Aβ(1−42) and Aβ(1−40), both of which form amyloid fibrils spontaneously, was examined. When 25 μM Aβ(1−42) was incubated with increasing concentrations of Aβ(1−40) (Lot No. 519599, Bachem AG), the time to proceed to equilibrium was concentration dependently extended (Figure 2A). Similarly, when 45 μM

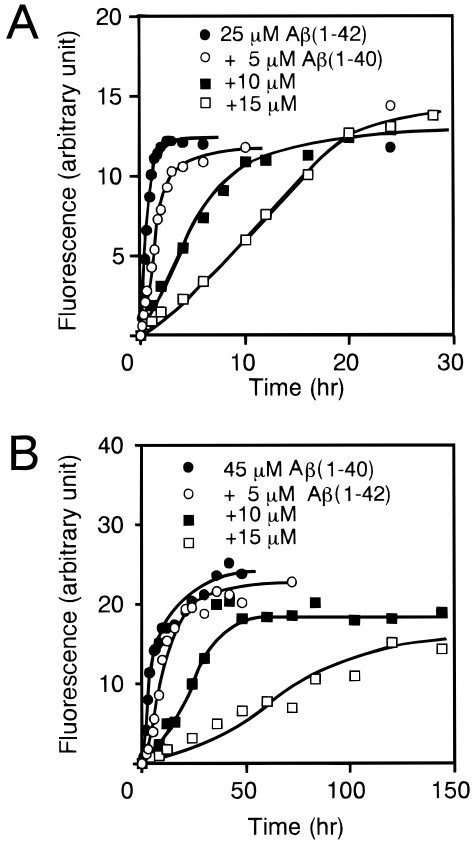

FIGURE 2: Interaction between Aβ(1−42) and Aβ(1−40) in the kinetics of fAβ formation. (A) Effect of fresh Aβ(1−40) in the kinetics of fAβ(1−42) formation from fresh Aβ(1−42). The reaction mixture contained 50 mM phosphate buffer, pH 7.5, 100 mM NaCl, 25 μM Aβ(1−42) and 0 (●), 5 (○), 10 (■), or 15 μM (□) Aβ(1−40) (Lot No. 519599, Bachem AG). The reaction was initiated by shifting the temperature to 37 °C as described under Experimental Procedures. At each incubation time, the reaction was stopped and analyzed by fluorescence spectroscopy as described under Experimental Procedures. (B) Effect of fresh Aβ(1−42) on the kinetics of fAβ(1−40) formation from fresh Aβ(1−40). The reaction mixture contained 50 mM phosphate buffer, pH 7.5, 100 mM NaCl, 45 μM Aβ(1−40) (Lot No. 519599, Bachem AG), and 0 (●), 5 (○), 10 (■), or 15 μM (□) Aβ(1−42).

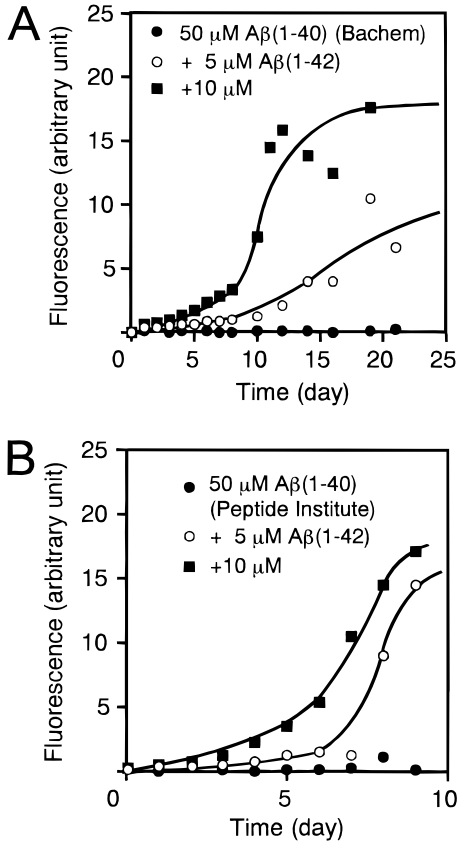

FIGURE 3: Interaction between Aβ(1−42) and nonamyloidogenic Aβ(1−40) in the kinetics of fAβ(1−40) formation. The reaction mixture contained 50 mM phosphate buffer, pH 7.5, 100 mM NaCl, 0.05% NaN_3, 50 μM Aβ(1−40) (A, Lot No. 518765, Bachem AG; B, Lot No. 480511, Peptide Institute, Inc.), and 0 (●), 5 (○), or 10 μM (■) Aβ(1−42). The reaction was initiated by shifting the temperature to 37 °C as described under Experimental Procedures. At each incubation time, the reaction was stopped and analyzed by fluorescence spectroscopy as described under Experimental Procedures.

Aβ(1−40) was incubated with increasing concentrations of Aβ(1−42), the time to proceed to equilibrium was concentration dependently extended (Figure 2B). In the former case, the final equilibrium level was independent of the Aβ(1−40) concentration added, while in the latter case, it decreased in a concentration-dependent manner with Aβ(1−42).

Then we examined the interaction between fresh Aβ(1−42) and nonamyloidogenic Aβ(1−40)s (Lot No. 518765, Bachem AG, and Lot No. 480511, Peptide Institute, Inc.), which do not form amyloid fibrils spontaneously but readily polymerize onto the ends of existing fibrils (see Figure 4B). The Aβ(1−40)/Aβ(1−42) ratio in cerebrospinal fluid is reported to be 16.5 ± 8.6 and 6.8 ± 3.3 for the AD group and age-matched normal group, respectively (*19*). Therefore, we added 5 or 10 μM Aβ(1−42) to 50 μM Aβ(1−40). As shown in Figure 3, the fluorescence showed a sigmoidal increase when 50 μM Aβ(1−40) was incubated with Aβ(1−42) at a molar ratio of 10:1 or 5:1 but not without Aβ(1−42). The lag time of the reaction was shortened with Aβ(1−42) in a concentration-dependent manner. Although the time to proceed to equilibrium was much longer than when an equal concentration of Aβ(1−42) (5−10 μM) was incubated without Aβ(1−40), the final equilibrium levels were much higher than those in the latter case (compare Figure 3 with Figure 1A). These results may indicate that Aβ(1−42) can initiate fAβ(1−40) formation from nonamyloidogenic Aβ(1−40).

Interaction between Aβ(1−42) and Aβ(1−40) in the Kinetics of fAβ Extension. When 25 μM fresh Aβ(1−42) (ultracentrifuged at 2×10^5 g) was incubated with 10 or 20 μg/mL (2.2 or 4.4 μM) of fAβ(1−42) at 37 °C, the fluorescence increased hyperbolically without a lag phase and proceeded to equilibrium much more rapidly than the case without fAβ(1−42) (Figure 4A). The initial rate of extension increased in a concentration-dependent manner with fAβ(1−42). Similar data were obtained when 50 μM fresh nonamyloidogenic Aβ(1−40) (Lot No. 518765, Bachem AG) was incubated with 10 or 20 μg/mL (2.3 or 4.6 μM) of fAβ(1−40) (Figure 4B).

We next examined the seeding effect of fAβ(1−42) on nonamyloidogenic Aβ(1−40). As shown in Figure 5A, when 50 μM Aβ(1−40) (Lot No. 518765, Bachem AG) was incubated with 10 or 20 μg/mL (2.2 or 4.4 μM) of fAβ(1−42), the fluorescence showed a sigmoidal increase. The lag time of the reaction was shortened by fAβ(1−42) in a concentration-dependent manner. The time to proceed

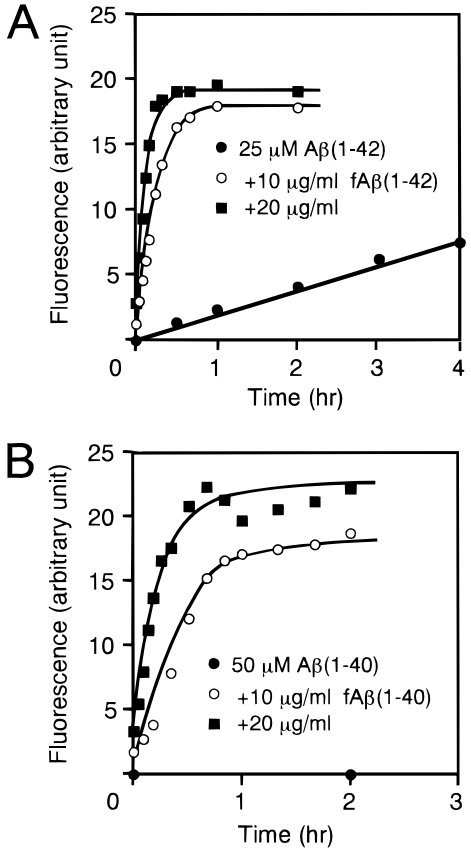

FIGURE 4: Extension of fAβ with homogeneous Aβ. (A) Kinetics of fAβ(1−42) extension with fresh Aβ(1−42). The reaction mixture contained 50 mM phosphate buffer, pH 7.5, 100 mM NaCl, 25 μM Aβ(1−42) (ultracentrifuged at 2×10^5 g), and 0 (●), 10 (○), or 20 μg/mL (■) (0, 2.2, or 4.4 μM) fAβ(1−42). The reaction was initiated by shifting the temperature to 37 °C as described under Experimental Procedures. At each incubation time, the reaction was stopped and analyzed by fluorescence spectroscopy as described under Experimental Procedures. (B) Kinetics of fAβ(1−40) extension with fresh Aβ(1−40). The reaction mixture contained 50 mM phosphate buffer, pH 7.5, 100 mM NaCl, 50 μM Aβ(1−40) (Lot No. 518765, Bachem AG), and 0 (●), 10 (○), or 20 μg/mL (■) (0, 2.3, or 4.6 μM) fAβ(1−40).

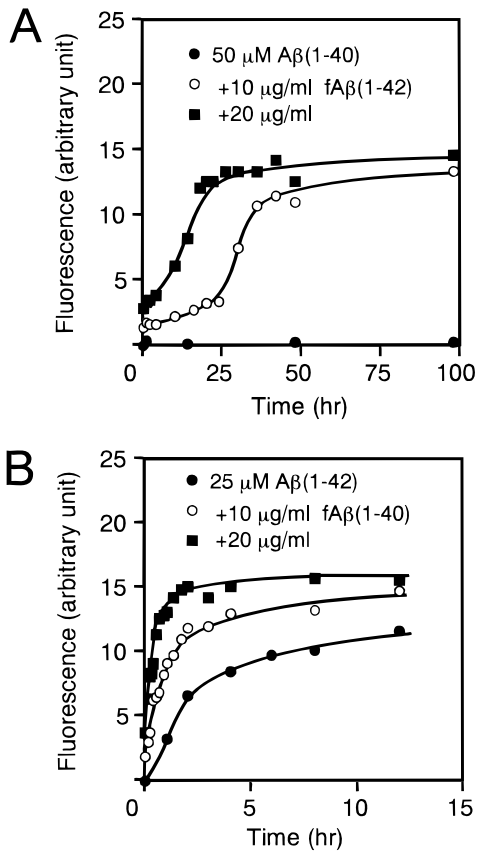

FIGURE 5: Extension of fAβ with heterogeneous Aβ. (A) Kinetics of fAβ(1−42) extension with fresh Aβ(1−40). The reaction mixture contained 50 mM phosphate buffer, pH 7.5, 100 mM NaCl, 50 μM Aβ(1−40) (Lot No. 518765, Bachem AG), and 0 (●), 10 (○), or 20 μg/mL (■) (0, 2.2, or 4.4 μM) fAβ(1−42). The reaction was initiated by shifting the temperature to 37 °C as described under Experimental Procedures. At each incubation time, the reaction was stopped and analyzed by fluorescence spectroscopy as described under Experimental Procedures. (B) Kinetics of fAβ(1−40) extension with fresh Aβ(1−42). The reaction mixture contained 50 mM phosphate buffer, pH 7.5, 100 mM NaCl, 25 μM Aβ(1−42) (ultracentrifuged at 2×10^5 g), and 0 (●), 10 (○), or 20 μg/mL (■) (0, 2.3, or 4.6 μM) fAβ(1−40).

to equilibrium was much longer than when an equal concentration of fAβ(1−40) was added to Aβ(1−40) (compare Figure 5A with Figure 4B). The final equilibrium level of fluorescence increase was independent of the concentration of fAβ(1−42). We also examined the seeding effect of fAβ(1−40) on fresh Aβ(1−42) (ultracentrifuged at 2×10^5 g), which forms amyloid fibrils spontaneously but proceeds to equilibrium much more slowly than those ultracentrifuged at 10^5 g (compare Figure 5B with Figure 1A). As shown in Figure 5B, when 25 μM Aβ(1−42) was incubated with 10 or 20 μg/mL (2.3 or 4.6 μM) of fAβ(1−40), the fluorescence increased hyperbolically without a lag phase and proceeded to equilibrium more rapidly than without fAβ(1−40). The initial rate of the reaction increased in a concentration-dependent manner with fAβ(1−40). The final equilibrium level of fluorescence increase was independent of the concentration of fAβ(1−40).

Then we examined the interaction between Aβ(1−42) and Aβ(1−40) in the kinetics of fAβ extension. As shown in Figure 6A, when 10 μg/mL (2.2 μM) of fAβ(1−42) and 15 μM Aβ(1−42) (ultracentrifuged at 2×10^5 g) were incubated with increasing concentrations of fresh Aβ(1−40) (Lot No. 519599, Bachem AG), the final equilibrium level was increased in a concentration-dependent manner. However, the initial rate of extension as well as the time to proceed to equilibrium were independent of the concentration of Aβ(1−40). As shown in Figure 6B, when 10 μg/mL (2.3 μM) of fAβ(1−40) and 40 μM Aβ(1−40) (Lot No. 519599, Bachem AG) were incubated with increasing concentrations of Aβ(1−42), the time to proceed to equilibrium as well as the final equilibrium level were independent of the concentration of Aβ(1−42) examined.

Electron Microscopic Observation of fAβ. As shown in Figure 7A, two types of amyloid fibrils were formed from the fresh Aβ(1−42) solution as described previously (*13*). Type A fibrils assumed the nonbranched filament structure of approximately 8 nm width. Although the helical structure was observed in some type A fibrils, it was not as distinct as that in the fAβ(1−40). Type B fibrils assumed the nonbranched filament structure of approximately 12 nm width and exhibited no helical structure. Seilheimer et al. (*20*) observed similar heterogeneity in the structure of fAβ(1−42) formed in vitro. As shown in Figure 7B, fAβ(1−40) formed from fresh Aβ(1−40) solution assumed

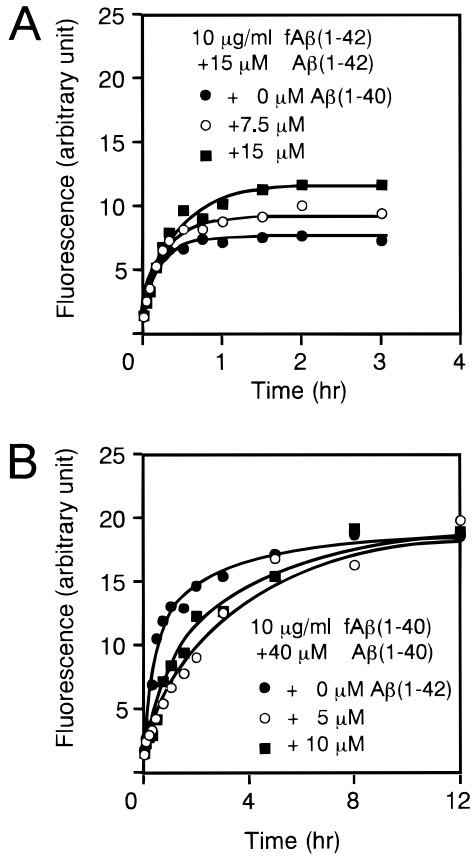

FIGURE 6: Interaction between Aβ(1−42) and Aβ(1−40) in the kinetics of fAβ extension. (A) Effect of fresh Aβ(1−40) on the kinetics of fAβ(1−42) extension with fresh Aβ(1−42). The reaction mixture contained 50 mM phosphate buffer, pH 7.5, 100 mM NaCl, 15 μM Aβ(1−42) (ultracentrifuged at 2×10^5 g), 10 μg/mL (2.2 μM) fAβ(1−42), and 0 (●), 7.5 (○), or 15 μM (■) Aβ(1−40) (Lot No. 519599, Bachem AG). The reaction was initiated by shifting the temperature to 37 °C as described under Experimental Procedures. At each incubation time, the reaction was stopped and analyzed by fluorescence spectroscopy as described under Experimental Procedures. (B) Effect of fresh Aβ(1−42) on the kinetics of fAβ(1−40) extension with fresh Aβ(1−40). The reaction mixture contained 50 mM phosphate buffer, pH 7.5, 100 mM NaCl, 40 μM Aβ(1−40) (Lot No. 518765, Bachem AG), 10 μg/mL (2.3 μM) fAβ(1−40), and 0 (●), 5 (○), or 10 μM (■) Aβ(1−42).

the nonbranched, helical filament structure of approximately 7 nm width and exhibited a helical periodicity of approximately 220 nm, as described previously (*12*).

When 25 μM fresh Aβ(1−42) was incubated with 10 μM amyloidogenic Aβ(1−40) (see Figure 2A), the major type of fibrils observed was fAβ(1−42) (Figure 7C). When 45 μM fresh amyloidogenic Aβ(1−40) was incubated with 10 μM Aβ(1−42) (see Figure 2B), the major type of fibrils observed was fAβ(1−40) (Figure 7D). When 50 μM fresh nonamyloidogenic Aβ(1−40) was incubated with 10 μM Aβ(1−42) (see Figure 3A), the major type of fibrils observed was fAβ(1−40) (data not shown). Although no increase in fluorescence was observed in the reaction mixture containing fresh Aβ(1−40) alone, small numbers of fAβ(1−40) were formed (data not shown).

When sonicated fAβ(1−42) or fAβ(1−40) was incubated with their constituents [i.e., Aβ(1−42) or Aβ(1−40)] (see Figure 4), no change was observed in their typical fibrillar structure (data not shown). When 20 μg/mL (4.4 μM) of sonicated fAβ(1−42) was incubated with 50 μM fresh Aβ(1−40) (see Figure 5A), the major type of fibrils observed was fAβ(1−40) (Figure 7E). Conversely, when 20 μg/mL (4.6 μM) of sonicated fAβ(1−40) was incubated with 25 μM fresh Aβ(1−42) (see Figure 5B), the major type of fibrils observed was fAβ(1−42) (Figure 7F).

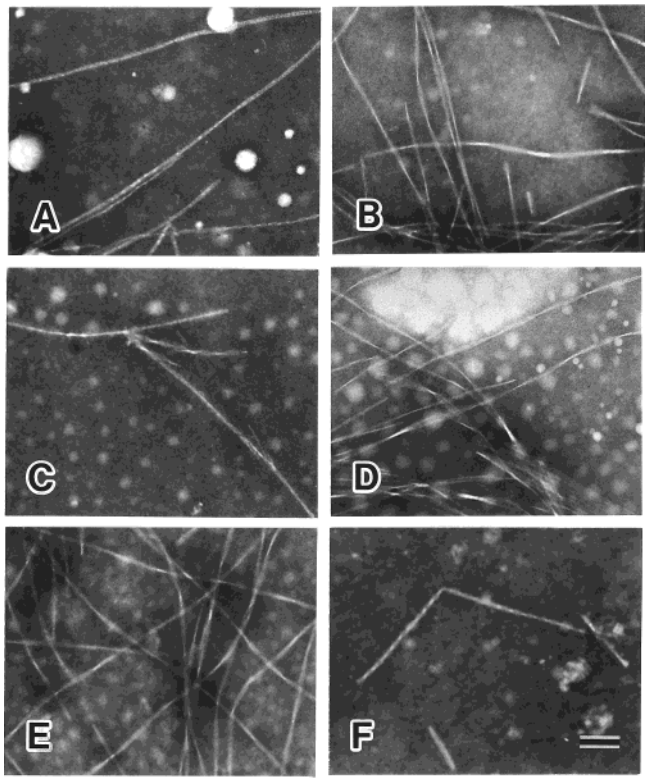

FIGURE 7: Electron micrographs of fAβs. The reaction mixtures containing 50 mM phosphate buffer, pH 7.5, 100 mM NaCl, and 25 μM Aβ(1−42) (A), 50 μM Aβ(1−40) (B), 25 μM Aβ(1−42) and 10 μM Aβ(1−40) (C), 45 μM Aβ(1−40) and 10 μM Aβ(1−42) (D), 20 μg/mL (4.4 μM) of fAβ(1−42) and 50 μM Aβ(1−40) (E), or 20 μg/mL (4.6 μM) of fAβ(1−40) and 25 μM Aβ(1−42) (F) were incubated and prepared for electron microscopy as described under Experimental Procedures. The bar indicates a length of 100 nm.

These findings indicate that the morphology of fAβ formed is governed by the major component of fresh Aβ peptides in the reaction mixture and not by the morphology of preexisting fibrils.

DISCUSSION

Amyloidogenicity of Aβ Peptides. We observed different amyloidogenicity between Aβ(1−42)s ultracentrifuged at 10^5 and 2×10^5 g as well as between two lots of Aβ(1−40)s (Lot No. 519599 vs Lot No. 518765). Although Soto et al. (*21*) reported that β-sheet content of Aβ(1−40)s correlates with their amyloidogenicity, CD spectrum analysis showed only a slight difference in the β-sheet content between Aβ(1−42)s ultracentrifuged at 10^5 and 2×10^5 g as well as between two lots of Aβ(1−40)s. As described in Experimental Procedures, no fibrillar components were observed in ultracentrifuged supernatant of Aβ(1−42) by electron microscopy. Therefore, it is not likely that contaminated fibrils would affect the amyloidogenicity of Aβ preparations. These results suggest that fresh Aβ preparations used in this study may contain immature Aβ complexes, which are invisible, nonfibrillar, and slowly sedimentable by ultracen-

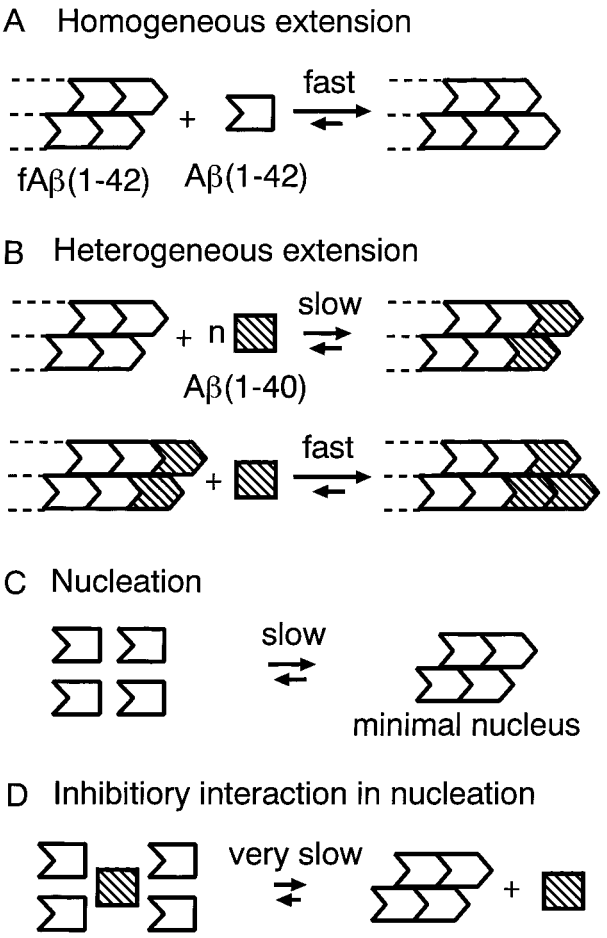

FIGURE 8: Hypothetical models of the interaction between Aβ(1−42) and Aβ(1−40) in the extension and nucleation reaction. (A) Kinetic model of the homogeneous extension (*12*). The extension of fAβ(1−42) proceeds via the consecutive association of Aβ(1−42) onto the ends of fAβ(1−42). This reaction is thermodynamically favorable. The extension of fAβ(1−40) can be explained by the same model. (B) Kinetic model of the heterogeneous extension. The association of Aβ(1−40) onto the ends of fAβ(1−42) would be thermodynamically unfavorable. After a certain number of Aβ(1−40) has polymerized onto the ends of fAβ(1−42), fAβ(1−40)-type ends would be formed, and then the association of Aβ(1−40) onto the ends would become thermodynamically favorable. (C) Kinetic model of the nucleation (*13*). Minimal nuclei would be formed by the cooperative association of n-meric Aβ(1−42). This reaction is thermodynamically unfavorable. (D) Inhibitory interaction between Aβ(1−42) and Aβ(1−40) in the nucleation reaction. Aβ(1−40) would interact with Aβ(1−42) and interrupt the conformational change of n-meric Aβ(1−42) into the minimal nucleus.

trifugation. The difference in the amount of these complexes may affect the amyloidogenicity of Aβ preparations. Further studies are essential to clarify the factors that affect the amyloidogenicity of Aβ preparations.

Interaction between Aβ(1−42) and Aβ(1−40) in the Kinetics of fAβ Extension. We previously reported that the extension of fAβ with their constituent Aβ follows a first-order kinetic model, where the fluorescence of ThT increases without a lag phase and proceeds to equilibrium hyperbolically (*12, 13*) (Figure 8A). On the basis of this model, we propose a model of the extension of fAβ with their nonconstituent Aβ. As shown in Figure 5A, fAβ(1−42) was able to nucleate fAβ(1−40) formation from nonamyloidogenic Aβ(1−40). However, the fluorescence increased sigmoidally with a lag phase. Jarrett et al. (*9*) observed a similar time-course curve. These time-course curves clearly indicate that the extension of fAβ(1−42) with Aβ(1−40) does not follow a first-order kinetics. Moreover, fAβ(1−40)-type fibrils were observed instead of fAβ(1−42)-type by electron microscopy (see Figure 7E). This heterogeneous extension of fAβ(1−42) with Aβ(1−40) could be explained as follows (see Figure 8B). First, fAβ(1−42) may initiate the polymerization of Aβ(1−40) onto the ends of fAβ(1−42). However, the complementarity between Aβ(1−40) and the ends of fAβ(1−42) may not be complete. Therefore, the association of Aβ(1−40) onto the ends of fAβ(1−42) would be thermodynamically unfavorable. After a sufficient number of Aβ(1−40) had polymerized onto the ends of fAβ(1−42), fAβ(1−40)-type ends would be formed, and further addition of Aβ(1−40) would be thermodynamically favorable.

When Aβ(1−42) was incubated with fAβ(1−40), the fluorescence increased hyperbolically without a lag phase and proceeded to equilibrium more rapidly than without fAβ(1−40) (Figure 5B). The electron microscopic observation also revealed that fAβ(1−42)-type fibrils were formed in the mixture (Figure 7F). The addition of fAβ(1−40) to Aβ(1−42) may also accelerate the formation of fAβ(1−42) by the association of Aβ(1−42) onto the ends of fAβ(1−40).

Interaction between Aβ(1−42) and Aβ(1−40) in the Kinetics of fAβ Formation from Fresh Aβ. As shown in Figure 2, the formation of fAβ from their fresh constituent was inhibited in a concentration-dependent manner with the nonconstituent Aβ. Electron microscopic observation revealed that the morphology of fAβ formed is governed by the major component of fresh Aβ in the reaction mixture (see Figure 7C,D). On the other hand, the extension of fAβ with their constituent Aβ was not inhibited by the nonconstituent Aβ (see Figure 6). These results may indicate that the inhibitory interaction of Aβ(1−42) and Aβ(1−40) would mainly take place in the nucleation process. Minimal nuclei would be formed by the association of n-meric Aβ(1−42) (see Figure 8C). The Aβ(1−40) added would interact with Aβ(1−42) and interrupt the conformational change of n-meric Aβ(1−42) into the minimal nuclei (see Figure 8D).

Quite inconsistent with the above-described inhibitory effect, when fresh Aβ(1−42) was incubated with nonamyloidogenic Aβ(1−40), fAβ(1−40) formation from nonamyloidogenic Aβ(1−40) was stimulated in a concentration-dependent manner with Aβ(1−42) (see Figure 3). This phenomenon could be explained as follows. Initially, the nucleation process of Aβ(1−42) would be interfered by Aβ(1−40). After a long lag time, a sufficient amount of nuclei could be accumulated, then the fibril extension would proceed by the consecutive association of Aβ(1−40) onto the ends of nuclei and existing fibrils. This scenario is based on the following results. First, when 10 μM Aβ(1−42) was incubated with nonamyloidogenic Aβ(1−40), the fluorescence of ThT proceeded to equilibrium much more slowly than when an equal concentration of Aβ(1−42) was incubated alone (compare Figure 1A and Figure 3). When fresh Aβ are incubated at 37 °C, the time to proceed to equilibrium is governed by the potential of spontaneous nucleus formation from fresh Aβ (*13*). Second, when 10 μM Aβ(1−42) was incubated with nonamyloidogenic Aβ(1−40), fAβ(1−40)-type fibrils were observed in the reaction mixture (data not shown).

Jarrett et al. (*9*) examined the ability of Aβ(26−43) to stimulate fAβ formation from Aβ(26−40). When 200 μM Aβ(26−40) or 20 μM Aβ(26−43) was incubated independently, no increase in turbidity was observed throughout the experiment. However, when 200 μM Aβ(26−40) was incubated with 20 μM Aβ(26−43), the turbidity was increased hyperbolically with no lag time. While we have no clear explanation for the difference in the time-course curves (sigmoidal vs hyperbolic), the amino-terminal truncation of Aβs [i.e., Aβ(1−42) vs Aβ(26−43) and Aβ(1−40) vs Aβ(26−40)] would have a critical effect on the interaction of Aβs with different C-terminal residues in the nucleation process.

The molecular mechanisms of the interaction between Aβ(1−42) and Aβ(1−40) need to be considered. The hydrophobic core of Aβ, i.e., residues 17−21, is reported to play an important role for the formation and stabilization of amyloid fibrils (*22*−*24*). This hydrophobic core would contribute to the association and binding of Aβ(1−42) and Aβ(1−40). The difference in the C-terminal residue is important for the conformation of Aβ, the potential of Aβ to form fAβ, and the morphology of fAβ formed (*25*). Therefore, the inhibitory interaction between Aβ(1−42) and Aβ(1−40) in the nucleation phase would be due to a minor difference in the conformation between Aβ(1−42) and Aβ(1−40) (see Figure 8D).

Biological Significance. It has been reported that Aβs, Aβ(1−42), Aβ(1−40), and other variants are produced simultaneously in vivo (*25*). Therefore, fAβ deposition in vivo would occur through the complex interaction among various Aβ species and other components [e.g., apolipoprotein E (apoE)]. The dose-dependent stimulatory effect of Aβ(1−42) to form fAβ(1−40) from nonamyloidogenic Aβ(1−40) (Figure 3) would be compatible with the increased production of Aβ(1−42) in the brain of various forms of FAD pedigrees (*2*). We and other groups have reported the inhibitory interaction of apoE with Aβ in the formation of fAβ in vitro (*13*, *26*−*28*). Very recently, this observation was supported by the evidence that expression of human apoE in the brain of a mouse model of AD reduces fAβ deposition in vivo (*29*).

In this paper, we demonstrated the interaction of different Aβ species on fAβ formation in vitro. This interaction is consistent with a nucleation-dependent polymerization model and may indicate the central role of Aβ(1−42) for fAβ deposition in vivo among the different coexisting Aβ species. We believe that the experimental system described in this paper may prove useful for the better understanding of fAβ deposition in vivo.

ACKNOWLEDGMENT

The authors thank C. Masuda, H. Okada, N. Takimoto, Y. Tanaka, and H. Takagi for excellent technical assistance.

REFERENCES

1. Selkoe, D. (1991) *Neuron 6*, 487−498.
2. Selkoe, D. (1996) *J. Biol. Chem. 271*, 18295−18298.
3. Rumble, B., Retallack, R., Hilbich, C., Simms, G., Multhaup, G., Martins, R., Hockey, A., Montgomery, P., Beyreuther, K., and Masters, C. L. (1989) *N. Engl. J. Med. 320*, 1446−1452.
4. Citron, M., Oltersdorf, T., Haass, C., McConlogue, L., Hung, A. Y., Seubert, P., Vigo-Pelfrey, C., Lieberburg, I., and Selkoe, D. J. (1992) *Nature 360*, 672−674.
5. Cai, X.-D., Golde, T. E., and Younkin, S. G. (1993) *Science 259*, 514−516.
6. Suzuki, N., Cheung, T. T., Cai, X.-D., Odaka, A., Otvos, L., Jr., Eckman, C., Golde, T. E., and Younkin, S. G. (1994) *Science 264*, 1336−1340.
7. St George-Hysrop, P., Haines, J., Rogaev, E., Mortilla, M., Vaula, G., Pericak-Vance, M., Foncin, J.-F., Montesi, M., Bruni, A., Sorbi, S., Rainero, I., Pinessi, L., Pollen, D., Polinsky, R., Nee, L., Kennedy, J., Macciardi, F., Rogaeva, E., Liang, Y., Alexandrova, N., Lukiw, W., Schlumpf, K., Tanzi, R., Tsuda, T., Farrer, L., Cantu, J.-M., Daura, R., Amaducci, L., Bergamini, L., Gusella, J., Roses, A., and Crapper Mclachlan, D. (1992) *Nat. Genet. 2*, 330−334.
8. Scheuner, D., Eckman, C., Jensen, M., Song, X., Citron, M., Suzuki, N., Bird, T. D., Hardy, J., Hutton, M., Kukull, W., Larson, E., Levy-Lahad. E., Vitanen, M., Peskind, E., Poorkaj, P., Schellenberg, G., Tanzi, R., Wasco, W., Lannfelt, L., Selkoe, D., and Younkin, S. (1996) *Nat. Med. 2*, 864−870.
9. Jarrett, J. T., Berger, E. P., and Lansbury, P. T., Jr. (1993) *Biochemistry 32*, 4693−4697.
10. Jarrett, J. T., and Lansbury, P. T., Jr. (1993) *Cell 73*, 1055−1058.
11. Harper, J. D., and Lansbury, P. T., Jr. (1997) *Annu. Rev. Biochem. 66*, 385−407.
12. Naiki, H., and Nakakuki, K. (1996) *Lab. Invest. 74*, 374−383.
13. Naiki, H., Hasegawa, K., Yamaguchi, I., Nakamura, H., Gejyo, F., and Nakakuki, K. (1998) *Biochemistry 37*, 17882−17889.
14. Lomakin, A., Chung, D. S., Benedek, G. B., Kirschner, D. A., and Teplow, D. B. (1996) *Proc. Natl. Acad. Sci. U.S.A. 93*, 1125−1129.
15. Lomakin, A., Teplow, D. B., Kirschner, D. A., and Benedek, G. B. (1997) *Proc. Natl. Acad. Sci. U.S.A. 94*, 7942−7947.
16. Esler, W. P., Stimson, E. R., Ghilardi, J. R., Vinters, H. V., Lee, J. P., Mantyh, P. W., and Maggio, J. E. (1996) *Biochemistry 35*, 749−757.
17. Reed, J., and Reed, T. A. (1997) *Anal. Biochem.* 254, 36−40.
18. Bradford, M. M. (1976) *Anal. Biochem. 72*, 248−254.
19. Kanai, M., Matsubara, E., Isoe, K., Urakami, K., Nakashima, K., Arai, H., Sasaki, H., Abe, K., Iwatsubo, T., Kosaka, T., Watanabe, M., Tomidokoro, Y., Shizuka, M., Mizushima, K., Nakamura, T., Igeta, Y., Ikeda, Y., Amari, M., Kawarabayashi, T., Ishiguro, K., Harigaya, Y., Wakabayashi, K., Okamoto, K., Hirai, S., and Shoji, M. (1998) *Ann. Neurol. 44*, 17−26.
20. Seilheimer, B., Bohrmann, B., Bondolfi, F., Müller, F., Stüber, D., and Döbeli, H. (1997) *J. Struct. Biol. 119*, 59−71.
21. Soto, C., Castaño, E. M., Kumar, R. A., Beavis, R. C., and Frangione, B. (1995) *Neurosci. Lett. 200*, 105−108.
22. Hilbich, C., Kisters-Woike, B., Reed, J., Masters, C. L., and Beyreuther, K. (1991) *J. Mol. Biol. 218*, 149−163.
23. Hilbich, C., Kisters-Woike, B., Reed, J., Masters, C. L., and Beyreuther, K. (1992) *J. Mol. Biol.* 228, 460−473.
24. Wood, S. J., Wetzel, R., Martin, J. D., and Hurle, M. R. (1995) *Biochemistry 34*, 724−730.
25. Teplow, D. B. (1998) *Amyloid: Int. J. Exp. Clin. Invest. 5*, 121−142.
26. Naiki, H., Gejyo, F., and Nakakuki, K. (1997) *Biochemistry 36*, 6243−6250.
27. Evans, K. C., Berger, E. P., Cho, C.-G., Weisgraber, K. H., and Lansbury, P. T., Jr. (1995) *Proc. Natl. Acad. Sci. U.S.A. 92*, 763−767.
28. Wood, S. J., Chan, W., and Wetzel, R. (1996) *Biochemistry 35*, 12623−12628.
29. Holtzman, D. M., Bales, K. R., Wu, S., Bhat, P., Parsadanian, M., Fagan, A. M., Chang, L. K., Sun, Y., and Paul, S. M. (1999) *J. Clin. Invest. 103*, R15−R21.

BI991161M